Genome-wide expression analysis of immune receptors in hot pepper reveals an autonomous NLR cluster in higher plants

Hye-Young Lee[a], Hyunggon Mang[a], Eun-Hye Choi[a], Ye-Eun Seo[a], Soohyun Oh[a], Saet-Byul Kim[a], Eunsook Park[b] and Doil Choi[a,c]

[a]Plant Immunity Research Center, Seoul National University, Seoul, 08826, Republic of Korea, [b]Department of Molecular Biology, College of Agriculture and Natural Resources, University of Wyoming, Laramie, WY 82071, USA, [c]Plant Genomics and Breeding Institute and Department of Plant Science, Seoul National University, Seoul, 08826, Republic of Korea

Corresponding Author: Doil Choi, doil@snu.ac.kr

Keywords: Plant NLR, Coiled-coil domain, Autoactivity, Singleton NLR, Cell death

Abstract

Plants possess hundreds of intracellular immune receptors encoding nucleotide-binding domain and leucine-rich repeat (NLR) proteins. Autoactive NLRs, in some cases, a specific domain of NLR, induce plant cell death in absence of pathogen infection. In this study, we identified a group of NLRs (G10) carrying autoactive coiled-coil (CC) domains in pepper (*Capsicum annuum* L. cv. CM334) by genome-wide transient expression analysis. The G10-CC-mediated cell death mimics the HR cell death triggered by interaction between NLR and effecter. Sequence alignment and mutagenesis analyses revealed that the intact form of α1 helix in G10-CC domain is critical for both G10-CC- and R gene-mediated HR cell death. We also found that G10-CCs are localized in plasma membrane as like the *Arabidopsis* singleton NLR ZAR1. Extended studies revealed that the G10-CCs in other *Solanaceae* plants including tomato, potato, and tobacco as well as a monocot plant, rice induce cell death by heterologous expression in *Nicotiana benthamiana*. Furthermore, the cell death induced by G10-CCs does not require known helper NLRs, implying that G10-NLRs are novel singleton NLRs. Our studies not only uncover the general function of CNL-induced cell death throughout mono- and dicot plants but also provides powerful resources to dissect the underlying molecular mechanism of NLR-mediated cell death in plants.

Introduction

Plants have evolved multiple immune receptors to activate defense responses against pathogen attack (1, 2). In the plant cell, nucleotide-binding and leucine-rich repeat (NLR) proteins monitor pathogen invasion by direct or indirect sensing of effectors delivered from pathogens (1).

After recognition, activated NLRs undergo conformational change and then initiate immune signaling (3, 4). Following NLR mediated immune activation, various defense responses are activated in the infected tissue, including calcium flux, production of reactive oxygen species (ROS), the activation of mitogen-activated protein kinases, biosynthesis/signaling of plant defense hormones and up-regulation of a subset of defense-related genes, which often associated with the hypersensitive response (HR), a type of programmed cell death (5, 6).

Genome-wide analyses have revealed that repertoires of NLRs are qualitatively and quantitatively diverse among plant species and they form distinct phylogenetic clusters (7). Although, a large effort during the last decades to understand the mechanism of NLR-mediated resistance has contributed to understanding the NLR classification based on their function in terms of immune signaling, how multiple NLR clades function in plant immune responses largely unknown.

In general, plant NLRs are classified following three different categories, singleton, pair and network NLRs based on their mode of action (7). Singleton NLRs function as a single genetic unit for both sensing and signaling (8-10). Singleton NLRs have the potential to confer resistance when expressed in heterologous plants, even taxonomically distant plants because no other host factors are required for its full activity (11). Additionally, singleton NLRs tend to possess a signaling domain which can induce visible cell death in heterologous plants. A second, paired NLR acts in pairs where the one works as ‘sensor' to detect pathogens, while the other functions as immune signaling 'executor' (12). Ectopic expression of executor NLR shows visible cell death without the perception of its cognate effector, which is referred to autoactivity (13, 14). The autoactivity of executor NLR is inhibited by co-expression of paired sensor NLRs, indicating that sensor NLR functions as a negative regulator of executor NLR in the absence of pathogen (13, 14). Sensor NLR in pair has an integrated domain which is an unusual additional domain to recognize effector proteins and then relieves the regulation of executor NLR, resulting in activation of immune responses. The typical NLR pairs are RESISTANCE TO RALSTONIA SOLANACEARUM 1 (RRS1)/RESISTANCE TO PSEUDOMONAS SYRINGAE 4 (RPS4) in *Arabidopsis thaliana* and RESISTANCE GENE ANALOG 5 (RGA5)/RGA4 in rice (*Oryza sativa*). These genes are genetically linked and orientated head-to-head to may share promoter for simultaneous regulation of transcription. Although an *in silico* analysis revealed that NLRs with integrated domain are common in higher plants, functional NLR pairs were discovered in few plant species (15). A third, more complex NLR model was reported as ‘NLR network’ mainly in Solanaceous plants. Helper NLRs, known as NLR-REQUIRED FOR CELL DEATH (NRC), are associated with phylogenetically linked sensor NLRs and have functional redundancies for conferring resistance against diverse pathogens (16).

NLR proteins are generally composed of three major domains, a variable N-terminal, a central nucleotide-binding (NB-ARC), and a C-terminal leucine-rich repeat (LRR) domain. In general, NLR genes are divided into two major groups based on the N-terminal domain (17, 18). One group contains the Toll/interleukin-1 receptor (TIR) domain at the N-terminus, referred as a TIR type-NLR (TNL), the other possesses the N-terminal domain with a coiled-coil (CC) structure, referred as a CNL type-NLR (CNL) (17). One of the CNLs carrying the N-terminal CC domains resembling *Arabidopsis* resistance protein RPW8 were considered as a distinct subclass RPW8-type CNL (RNL) based on their function in the downstream signaling (19-21). RNLs are highly redundant in plant species and necessary for the function of other NLRs (21). One of RNL genes, N REQUIREMENT GENE 1 (NRG1) is specific to TNL mediated immunity and partially contributes to the signaling of some CNLs (22). The other RNLs, ADR1s are also known to associate with various TNLs and CNL signaling (20).

Structural analyses of NLR proteins have revealed that the N-terminal domain plays multiple regulatory roles. In the case of several NLRs, N-terminal domain physically interacts with host target proteins which are manipulated by effector proteins (23-26). Besides, interaction between homotypic N-terminal domains contribute to form the high-order complex of NLRs upon activation (27-29). Moreover, the N-terminal domain of NLRs is also involved in transducing cell death signal. Overexpression of the N-terminal region of a few NLRs is sufficient to triggers cell death without cognate effector proteins (19-21, 28-31). However, it remains unclear how the CNLs are activated and trigger cell death.

Recently, it has been reported that the reconstitution of the inactive and active complexes of *Arabidopsis* CNL, HOPZ-ACTIVATED RESISTANCE1 (ZAR1) with receptor-like cytoplasmic kinases (RLCKs) by structural and biochemical approaches (4, 32). Cryo-electron microscopy structures showed that activated ZAR1 forms a wheel-like pentamer resistosome and then undergoes a conformational change to expose a funnel-shaped structure formed by the N-terminal α1 helix of the CC domains. They suggested that the exposed α1 helix of the ZAR1 resistosome mediates cell death by translocating into the plasma membrane (PM) and perturbing membrane integrity (32). However, whether the ZAR1 model is sufficient to explain CC-induced cell death is not evident and need to be elucidated.

The Solanaceous plants belong to a large family that consists of over 3,000 species encompassing economically important crops such as potato (*Solanum tuberosum*), tomato (*Solanum lycopersicum*), and pepper (*Capsicum annuum*) (33). Previous comparative analysis of NLR genes across Solanaceae genomes revealed that the NLR gene family is classified into one TNL and 13 CNL subgroups (34). Pepper CNL-Group 10 (G10) is composed of 34 members including known disease resistance genes (R gene) *Pvr4* and *Tsw* conferring resistance to Potyvirus such as *Potato virus* Y (PVY) and *Tomato spotted wilt virus* (TSWV) by the recognition of a viral effector (35, 36). Structural domain analysis revealed that the CC domain of Pvr4 is sufficient to activate cell death in the absence of the viral effector NIb (37).

Here, we report that the CC domains of G10-NLRs (G10-CCs) in pepper specifically induced HR-like cell death through genome-wide screening in *Nicotiana benthamiana*. Autoactive G10-NLRs and G10-CCs-mediated cell death were associated with immune responses, G10-CC domains are localized in PM and α1 helix of the G10-CC domains is critical to mediate cell death. Cell death induced by autoactive G10-NLRs and G10-CCs were not compromised in *NRC*s- or *NRG1*/*ADR1*-silenced plants, suggesting that helper NLRs are not required for G10-NLR-mediated cell death signaling. Surprisingly, G10-CCs in other Solanaceae plants, tomato, potato and tobacco as well as a monocot plant, rice induce cell death in *N. benthamiana*. We propose that G10-NLRs are novel singleton NLR subfamily and G10-CCs could serve as powerful resources to dissect the underlying molecular mechanism of NLR-induced plant cell death.

Results

The CC domains of pepper G10-NLRs induce cell death in *N. benthamiana*

In the previous study, intact pepper NLRs were identified and assigned into 15 groups including 1 TNL and 14 CNLs (34). To identify the autoactive NLRs at a genome-wide scale, genomic fragments of 436 intact pepper NLRs were cloned into binary vector pCAMBIA2300-LIC (35, 36). The sequences of all inserts were confirmed by Sanger sequencing (Dataset S1) and the constructs were transiently expressed in *N. benthamiana* leaves by agroinfiltration. Among the tested 436 NLRs, only fifteen NLRs (3.4%) triggered cell death (Table 1) and randomly distributed into six groups, TNL, CNL-G5, CNL-G9, CNL-G10, CNL-G11, and CNL-NG. To verify whether these genes function as an executor NLR with their paired sensor NLRs, we examined the upstream flanking gene of the autoactive NLRs using pepper chromosome pseudomolecules because many NLR pairs are genetically linked in head-to-head orientation (38, 39). Although nine out of fifteen autoactive NLRs have an NLR-type gene at the upstream flanking region, none of them was arranged in a head-to-head orientation (Table S1). Furthermore, these upstream NLR genes do not contain the sequences coding an integrated decoy domain which is a typical feature of sensor in paired NLRs. These results suggest that the conventional paired NLR immune receptors, like *Arabidopsis* RPS4/RRS1 pair and rice RGA4/RGA5 pair, probably do not exist in pepper. Previous studies reported that the N-terminal TIR or CC domain from a specific set of resistance proteins, mostly potential singleton NLRs, induce cell death when overexpressed alone in plants (21, 40, 41). These results suggesting that NLR proteins normally trigger immune signaling via their N-terminal domain. To identify NLRs carrying an autoactive N-terminal domain (NTD) in pepper, a representative subset of NTDs including those of autoactive NLRs were transiently overexpressed in *N. benthamiana* in the same way as full-length NLR. The representative NTDs for each group were randomly chosen more than 15% of all assigned NLRs from a subclade in phylogenetic tree analysis (Dataset S2). The NTD fragments were determined the entire N-terminus up to the predicted P-loop in the NB-ARC domain. Of 15 autoactive full-length NLRs, only two TIR domains and three CC domains from autoactive TNLs and G10-NLRs, respectively showed visible cell death when expressed in *N. benthamiana* (Table S2). Among CNL-NG, CC domains from pepper homologs of NbNRG1 and

NbADR1 trigger cell death. In particular, the tested CC domains of CNL-G10 (hereafter G10-CCs) in pepper trigger cell death in a significantly higher proportion (70.8%) than those of other groups (Table 1 and *SI Appendix*, Fig. S1). G10-NLRs form a distinct cluster in the phylogenetic tree and include several cloned functional R genes, *Pvr4*, *Tsw* in pepper and *RPS2* and *RPS5* in *Arabidopsis* (*SI Appendix*, Fig. S2) (34). Although G10-NLRs belongs to conventional CNLs, G10 is phylogenetically separated from other CNL clades (*SI Appendix*, Fig. S2) (34). Taken together, these data suggest that G10-NLRs have specific features from other CNLs and may indicate its unique role(s) in plant immunity.

CC-induce cell death mimics R gene-mediated HR

We next investigated whether cell death induced by autoactive G10-NLRs or G10-CCs is engaged in R gene-mediated defense responses against pathogen. An autoactive, CC309, a non-autoactive, CC10-1, and an autoactive full-length NLR, NLR620 were used in this assay. A known G10-NLR gene, *Pvr4* and its cognate Avr gene, *NIb* of *Pepper mottle virus* were also included as a positive control for R gene-mediated defense responses (36). Even though sharing high identity (95.5% and 89.9% at the nucleotide and amino acid level, respectively), CC309 and CC10-1 showed the opposite phenotype (Fig. 1A). Transient overexpression of CC309 and NLR620, but not CC10-1, triggered visible cell death in *N. benthamiana*. All proteins were detected by immunoblotting (Fig. 1B). Expression level of CC10-1 was much lower than that of CC309. To exclude the possibility that low protein accumulation contributed to the non-functionality of CC10-1, a green fluorescent protein (GFP) was fused to CC309 and CC10-1 at C-terminus. Although CC309-GFP and CC10-1-GFP were accumulated to similar level, CC10-1-GFP still did not trigger cell death, indicating that low protein level of CC10-1 does not account for its non-autoactivity (*SI Appendix*, Fig. S3).

At 2 days after agroinfiltration, we examined hydrogen peroxide accumulation in leaves using 3,3'-diamino benzidine hydrochloride (DAB) staining. H_2O_2 production was observed in progress of cell death by activated Pvr4 (Fig. 1C). As shown by Pvr4, cells expressing CC309 and NLR620 but not CC10-1 showed accumulation of hydrogen peroxide. These results indicate that accumulation of reactive oxygen species, one of defense responses against pathogen infection, is accompanied by the cell death induced by autoactive G10-NLR and G10-CC.

To verify the ectopic expression of autoactive G10-NLR and G10-CC mimic activation of defense-related gene, transcript accumulation of four defense-related genes was monitored during the progress of cell death by CC309 and NLR620 at various time points after agroinfiltration (Fig. 1D). In overexpression of CC309 and NLR620 but not CC10-1, significantly higher transcript levels of an HR cell death marker gene, *Harpin-induced 1* (*Hin1*), the transcription factor of physiological substrate of mitogen-activated protein kinases, *WRKY8* and a cytochrome P450 involved in sesquiterpene phytoalexin biosynthesis, *CYP71D20*, and *Pathogenesis-related gene 1* (*PR1*) were detected (42-45). As a result, cell death induced by autoactive G10-NLR and G10-CC is also correlated with the accumulation of defense-related gene transcripts.

Although ROS production and upregulation of defense-related genes are typical immune responses, we cannot exclude that they also occur as the consequence of cell death. We performed to verify that autoactive G10-NLR and G10-CC indeed trigger defense response by co-expression with a Potato Virus X (PVX) vector carrying a GFP (37) . We hypothesized that if autoactive G10-CC- or G10-NLR-mediated cell death is associated with defense responses, replication of PVX would be suppressed in co-expressed cells. To avoid the chance that cell death affects the replication of PVX, The GFP signal was monitored before the onset of severe cell death phenotype (*SI Appendix*, Fig. S3). Compared with empty vector (EV), autoactive CC domain of Pvr4 and Pvr4 significantly reduced the abundance of PVX:GFP. Moreover, the GFP accumulation was also almost completely inhibited by expression of CC309 and NLR620 (Fig. 1E, 1F). Taken together, cell death induced by autoactive G10-NLR and G10-CC functionally mimics R gene-mediated HR cell death.

The N-terminal α1 helix is critical for autoactivity of G10-CCs

We performed an alignment analysis of the pepper G10-CCs to identify a conserved motif for cell death activity. However, none of a conserved motif is found across all G10-CCs (*SI Appendix*, Fig. S5). Phylogenetic analysis based on amino acid sequences of pepper G10-CCs revealed that they are divided into three subclades with 100% bootstrap confidence level (Fig. 2A). In the phylogenetic analysis, we found that most of non-autoactive G10-CCs (shown by open circle) belong to subclade I (Fig. 2A left panel). It has been recently reported that the N- terminal α1 helix of the ZAR1 CC domain is crucial for its cell death-inducing activity based on the crystal structure model (32). It prompted us to further analysis the α1 helix of subclade I. Prediction of secondary structure analysis using JPRED4 (http://www.compbio.dundee.ac.uk/jpred4) revealed that non-autoactive G10-CCs (CC292, CC310, CC368 and CC430) in subclade I have shorter α1 helix than autoactive G10-CCs (Fig. 2A, right panel) and partial deletion on α1 helix was found in non-autoactive G10-CCs (Fig. 2B). Although non-autoactive CC474 has a relatively sufficient length of α1 helix, deletion was found in the linker region between α1 and α2 helix (Fig. 2A right panel and 2B), suggesting that the deletion may disrupt the formation of appropriate structure to be required for their activity. Taken together, these results imply that cell death activity of non-autoactive G10-CCs in subclade I attributed to deficiency of proper α1 helix structure.

Interestingly, CC10-1 in subclade III is only non-autoactive CC domain although having a sufficiently long α1 helix. Alignment with CC309 revealed that sequence variation was mainly observed in the N-terminal 12 aa region (Fig. 3A, *SI Appendix*, Fig. S5). It has been reported that an N-terminus of CC domain in NLRs is important to not only cell death activity, but also subcellular localization of NLR protein (32, 46). In the case of Arabidopsis *RPS5*, one of known resistance genes in G10, N-terminal acylation-mediated plasma membrane (PM) localization is essential for their cell death activity, although the RPS5 CC domain also requires the NB-ARC domain to trigger cell death (46). However, pepper G10-CCs do not contain predicted S-acylation site at N-terminus. Meanwhile, the

transmembrane region in 1-30 aa region of CC309, but not CC10-1, was predicted by TMHMM Server v. 2.0 with a low probability (*SI Appendix*, Fig. S6). We hypothesized that sequence variation in α1 helix between CC309 and CC10-1 has an effect to their subcellular distribution, and consequently affects the difference in their ability. We checked the subcellular distribution of G10-CCs-GFP in *N. benthamiana* using the confocal microscope. GFP signals of CC309-GFP and CC10-1 were detected at the PM and colocalized with FM4-64, a fluorescence dye specific for PM (Fig. 3B). Moreover, another non-autoactive G10-CCs in subclade I and subclade II were also localized at PM (*SI Appendix*, Fig. S7). These results suggest that non-autoactivity of G10-CCs is not attributed by mislocalization to other cellular compartments.

This observation led us turning back to N-terminus of subclade III, we found that well conserved 'TAILSP' motif in subclade III except CC10-1 (*SI Appendix*, Fig. S5). To confirm the function of this motif in autoactivity, we generated the CC309 mutants which are replaced in 1 to 12 aa or partial region with those of CC10-1 (Fig. 3C) and expressed in *N. benthamiana*. As a result, substitution in 7 to 12 aa ($mCC309^{7-12}$), corresponds to 'TAILSP' motif, as well as in 1 to 12 aa ($mCC309^{1-12}$), but not 1-6 aa ($mCC309^{1-6}$), abolished their cell death-inducing activity (Fig. 3D). Conversely, the $mCC10\text{-}1^{5-10}$ carrying 7-12 aa of CC309 slightly recovered the activity, indicating that 7-12 aa region of CC309 is critical for autoactivity. To confirm 'TAILSP' motif is also critical for R gene-mediated cell death, this motif of CC_{Pvr4} and Pvr4, note that CC_{Pvr4} is CC322 in our classification, were mutated to those of CC10-1. Like CC309, mutation of TAILSP motif resulted in the disruption of the cell death-inducing activity of CC_{Pvr4} when even expressed with its cognate effector NIb (Fig. 3E). Immunoblots showed comparable expression levels of these protein fragments (Fig. 3G, 3H). These results suggest that TAILSP of α1 helix is crucial for autoactivity of G10-CCs and R gene.

Next, to identify the amino acids responsible for functionality, site-directed mutagenesis using synthetic oligonucleotides was performed to exchange each residue in TAILSP motif to alanine or glutamate. A8, I9 and L10 were substituted with negatively charged glutamate (E) and T7, S11 and 12P were exchanged to alanine (A). Mutation of A8E substantially reduced the activity and those of I9E and L10E completely disrupt their function (Fig. 3F), indicating that hydrophobic residues are essential for cell death-inducing activity. All of the mutant proteins accumulated to similar levels, except for L10E, when expressed in *N. benthamiana* leaves indicating that the observed loss-of-function phenotypes were not due to protein destabilization (Fig. 3I). Together, our results suggest that hydrophobic amino acids at the α1 helix of pepper G10-CC are critical for autoactivity.

Four α helices of G10-CC are required for cell death-inducing activity

It has been reported that only 29 amino acids of NRC4 is sufficient to induce cell death in *N. benthamiana* (47). To define the minimal region of G10-CC to be sufficient for autoactivity, we found that G10-CC domain has five α helices on their N-terminus through secondary structure analysis and generated the N-terminal or C-terminal deletion mutants of CC309 (Fig. 4A). The truncated fragments of CC309 with five (N1) or ten (N2) amino acid deletion at the N-terminus showed diminished cell death phenotype (Fig. 4B). C-terminal deletion mutants C1 and C2, but not C3, induced cell death (Fig. 4B and D), suggesting that the four α helices of the G10-CC are necessary and sufficient to trigger cell death. The capacity for cell death was quantitatively measured as the photosynthetic parameters, quantum yield of photochemistry in PSII (Fv/Fm) (Fig. 4D) (48). We performed the immunoblot analysis to check the protein accumulation of all the FLAG-fused deletion mutants after 24 hr agroinfiltration. N1 and N2 proteins were accumulated much lower levels than full-length of CC309, suggesting that N-terminus may be associated with the protein stability. However, C2 showed lower protein accumulation than C1, nevertheless gave the strongest cell-death and lowest Fv/Fm (Fig. 4B, C, and D), indicating that protein levels do not affect the cell death and α5 helix is not essential component for autoactivity. Consistent with previous observation in motif-swap experiments, these results implied that α1 helix is critical to cell death-inducing activity of G10-CC and at least four α helices are required for their autoactivities.

Cell death mediated by G10-CCs is independent of helper NLRs

Recent studies revealed that NLR-mediated immunity have complicate network and many NLRs require helper NLRs for their activity in immune response (16), we tested the dependency of the G10-NLR and G10-CC-mediated cell death on known helper NLRs. We performed virus-induced gene silencing (VIGS) to simultaneously co-silence the RNL-type helpers, *NbNRG1* and *NbADR1*, and *NRC*-type helpers, triple NRCs (NRC2, 3, 4) respectively. Autoactive G10-CCs were expressed in silenced plants by agroinfiltration (Fig. 5A). The silencing efficiency was estimated by qRT-PCR analysis of the transcript levels of each gene at 3 weeks after VIGS (Fig. 5C). One of *NbNRC*-dependent *Phytophthora infestans* resistance gene, *R8* and its cognate effector *Avr8* were used as control (16). In NRCs-silenced plants, cell death mediated by *R8*/*AvrR8* was compromised, whereas those mediated by autoactive CC309, and NLR620, and Pvr4/NIb were not (Fig. 5A). Besides, cell death induced by G10-CC and G10-NLR was also not compromised in *NRG1* and *ADR1*-silenced plants (Fig. 5A, B). These results indicate that G10-CCs and G10-NLR trigger cell death by helper-independent manner.

G10-CC domains of other plant species induce cell death

Next, we tested the commonality of the G10-CC-medicated cell death in other plants. Because being the only conserved domain of NLR proteins to capable of sequence alignment, the NB-ARC domains of 1661 NLR proteins from four Solanaceous species (pepper, tomato, potato, and tobacco), a monocot plant rice and a Brassicaceae plant *Arabidopsis thaliana* were used for phylogenetic analysis (*SI Appendix*, Fig. S2). Subclades were grouped into fifteen groups by comparing with the previous study for classification of Solanaceae NLRs (34). The 124 NLR proteins clustered G10-NLRs in the phylogenetic tree. Subsequently, representative G10-CCs from five plant species (pepper, tomato, potato, tobacco and rice) were also randomly chosen from a subclade in

phylogenetic tree. More than 40% tested G10-CCs from Solanaceae plants and even taxonomically distant rice plant, trigger cell death in *N. benthamiana* (Fig. 6A, *SI Appendix*, Table 3). In addition, a recent finding showed that N-termini containing a predicted CC domain of nearly all of the CNLs in *Arabidopsis thaliana* ecotype Columbia-0 triggered cell death (49). All of CNLs from group B, except At1g63360, in Wro´blewski *et al*. belong to G10-NLRs according to our classification and 15 of 23 G10-CC domain fragments induce cell death in *Arabidopsis* (49). Combined with this report, our results indicate that the G10-CCs of not only Solanaceae plants, but also evolutionally distant rice enable to trigger cell death.

Discussion

In plants, NLR proteins are one of the largest and widespread family of intracellular immune receptors and activate potent immune responses, which often accompany hypersensitive response. In this study, we show that G10 is major NLRs having autoactive NTDs among the 15 NLR groups in pepper. The autoactive G10-CC induced cell death resembles R gene-mediated HR and immune responses, suggesting that G10-NLRs be able to trigger immune signaling. Sequence analysis of pepper G10-CCs discovered that non-autoactive CCs contain partial deletion or variation in their α1 helix region and 'TAILSP' motif is critical for their cell death activity. Four α helices of G10-CC are minimum requirement for autoactivity. Furthermore, cell death mediated by G10-CCs is independent of helper NLRs. Remarkably, G10-CCs of other plant species, Solanaceae and non-Solanaceae plants, induce cell death in *N. benthamiana*.

Some NLRs function as sensor/signaling pair. Sensor NLR comprises additional unusual non-conserved domains to recognize the pathogens and is coupled with a helper NLR (also known as executor) to initiate immune signaling (12). The Sensor NLR forms heterodimerization with executor NLR to suppress its autoactivity without the perception of pathogen (13, 14). The recognition of pathogen by sensor NLR resulted in releasing executor NLR from inactive state to active state. Generally, NLR pairs are genetically linked and orientated head-to-head may sharing promoter for simultaneous regulation of transcription (15, 50). We discovered that autoactive G10-NLRs do not exist in head-to-head orientation in their upstream region and also do not contain the additional integrated domain (*SI Appendix*, Table S1). Although, genome-wide analysis using updated pseudomolecules of pepper revealed that 19 NLR pairs exist head-to-head orientation in pepper (38). Only one G10-NLR (referred to CaNBARC403) was identified, however CaNBARC403 does not have autoactivity and additional domain on its upstream flanking gene (*SI Appendix*, Table S4). These data support that autoactive G10-NLRs in pepper may not play a role as an executor in NLR pairs and also their activity is probably regulated by negative regulatory protein(s) not NLRs in inactive state such as RPS2 regulated by RIN4 (51). Conclusively, the conventional paired NLR appears not exist in pepper G10-NLRs.

Here we proposed that pepper G10-NLRs are a new putative singleton NLR clade based on several pieces of evidences. First, we observed that many G10-CCs from Solanaceae plants including pepper, potato, and tomato trigger autoactivity in *N. benthamiana* (Table1, *SI Appendix*, Table S3 and Fig 6.). In addition, a recent finding showed that 15 of 22 CC-NLRs in group B, belong to G10 in our classification, triggered cell death in *Arabidopsis* (49). Taken together, G10-CCs in Solanaceae and Brassicaceae have the potential to trigger cell death (*SI Appendix*, Table S3). Second, G10-CCs from taxonomically distant plants trigger visible cell death in *N. benthamiana*. We show that G10-CCs in monocot rice induce cell death in *N. benthamiana*, although the strength of cell death were relatively weak compared to other Solanaceae G10-CCs (Fig 6, *SI Appendix*, Table 3). Besides, 13 or 5 out of 22 *Arabidopsis* G10-CCs showed visible cell death in *N. benthamiana* and lettuce, respectively (49). Third, functional analysis of known R genes in G10-NLRs reported that G10-NLRs are responsible for sensing of each cognate effector protein(24, 37). Moreover, the CC domain of functional G10-NLR, RPS5, plays an important role in the recognition of its cognate effector AvrPphB (24). Previously we have reported that the LRR domain of Pvr4 is important to recognize PepMoV-NIb by domain-swap experiment with susceptible allele of Pvr4 (37). Taken together, G10-NLRs function in effector recognition as well as initiation of immune signaling. Lastly, it is also supported by the finding that sustainable cell death mediated by G10-CC or G10-NLR in helper NLRs-silenced plants such as RNLs and NRCs (Fig. 5). Moreover, G10 is NRC independent clade in phylogenetic tree analysis (*SI Appendix*, Fig. S2). However, it is a doubt that all G10-NLRs across plant species shares the same mechanism to confer resistance. Because helper NLRs, *ADR1* and *NRG1*, are completely or partially required for *RPS2* mediated cell death (22). Interestingly, we observed that *RPS2* also induce cell death in helper NLRs-silenced *N. benthamiana* (unpublish data). Therefore, an alternative scenario is that G10-NLRs do not require other NLR genes to function in evolutionary distant plants or downstream signaling components for G10-mediated cell death were well conserved in a wide range of plant species. Recently, Adachi et al., proposed that NLRs may have evolved from multifunctional singleton receptors to functionally specialized and diversified receptor pairs and intricate receptor networks (8). Interestingly, the end of our research stage, Seong *et al*. reported that tomato's G10-NLRs did not go through duplication events after a relatively ancient one compared with other group NLRs (52). It should be noted that their G10 of tomato is the same classification with our pepper G10-NLR.

In this study, pepper G10-CCs have autoactivity with an exclusively high proportion of tested CC-domains compared to other groups (Table 1). However, G10-NLRs are not the only group containing autoactive CC domains. It was reported that transient overexpression with the tomato or tobacco CC domain of I2-like NLR induce cell death in *N. benthamiana*, but never with the CC domain of the pepper I2-like NLRs (31). Interestingly, C-terminal tagging with enhanced yellow fluorescent protein (eYFP) at CC domain of pepper I2-like NLR (note that the pepper I2-like NLRs belong to G4) triggers strong cell death upon transient overexpression in *N. benthamiana*. This tag-dependent autoactivity has been observed in several CC domains of NLRs regardless of the level of protein accumulation (31). The GFP and YFP are known to have a weak dimerization tendency, which might have affected their autoactivity. These results imply that pepper G4-NLRs

may have evolved differently for the CC domain to require additional domain(s) for oligomerization to trigger immune signaling after speciation and G4-NLR and G10-NLR appear to behave mechanistically differently in terms of inducing cell death.

Sequence analysis of pepper G10-CCs showed that partial deletion or variation is present in the α1 helix region in non-autoactive CCs (Fig. 2 and *SI Appendix*, Fig. S3) and mutation in α1 helix of G10-CC or G10-NLR compromised their cell death activity (Fig. 3). This region is matched with ZAR1 α1 helix forming funnel-shaped structure in the PM after conformational switch during activation of the ZAR1 resistosome and Amphipathic residues in ZAR1 α1 helix are essential for the cell death activity (32, 47). Taken together, α1 helix is important to trigger cell death for singleton NLRs. However, α1 helix of pepper G10-CCs was required for their cell death activity but does not affect PM localization. It would be interesting to test in the future if pepper G10-CCs or G10-NLRs form multimerization like Zar1 resistosome to understand the general mechanism of NLR induced cell death. Here we propose that G10-NLRs not only serve as valuable resources to understand the molecular basis of NLR-mediated cell death but also provide a critical information for identification of new disease resistance genes in crop plants.

Materials and Methods

Plant Materials and Growth Condition

N. benthamiana plants were grown in horticultural bed soil (Biogreen, Seoul Bio Co., Ltd., Seoul, Korea) under a well-maintained chamber with 16-/8hr photoperiod, temperature of 25°C, PPFD 80-100 µmol m^{-2} sec^{-1} and relative humidity of 70%. Four-week old plants were used for transient overexpression. For VIGS experiments, foliage leaves of 2-week old plants were inoculated with *Agrobacterium*.

Identification of NLRs and phylogenetic tree analysis

Predicted protein sequences from reference genomes of tomato, and tobacco (http:// solgenomics.net/) and rice (http://rice.plantbiology.msu.edu/) were used in this study. The group information and the sequences of intact NLR genes in pepper, tomato and potato were derived from Seo et al., 2016 (34). For identification of G10-NLRs in tobacco, rice and *Arabidopsis*, predicted proteins containing the NB-ARC domain (PF00931) over 160 amino acids were extracted. To classify these NLR genes, NB-ARC domains were used for and orthoMCL clustering and phylogenetic tree construction with the those of Solanaceae NLR proteins. In phylogenetic tree and orthoMCL clustering, the NB-ARC domains that are clustered with the those of Solanaceae G10-NLRs were assigned to G10. For phylogenetic tree analysis for NLRs in six plant species, amino acid sequences of NB-ARC domains were used for construction.

Plasmid constructions

The fragments of pepper NLRs were amplified from genomic DNA of *Capsicum annuum* L. cv Criollo de Morelos 334 (CM334) based on annotation of pepper reference annotation v.1.55 (53). To amplify target genes, the primers were specifically designed within 1 kb of 5' or 3' UTR region for each gene. The amplicons were cloned in the pCAMBIA2300-LIC vector containing cauliflower mosaic virus 35S promoter and nopaline synthase terminator by ligation-independent cloning (LIC) method (36, 54). The N-terminal domain of NLRs were defined from methionine to just before p-loop motif in NB-ARC domain. Amplified NTD fragments were put into pCAMBIA2300-LIC or pCAMBIA2300-3xFLAG-LIC vector in the same way as full length NLRs. For cloning of CC domains from other plant species, the fragments were amplified from genomic DNA of rice (*Oryza sativa* L. cv. Nakdong) and tobacco (*Nicotiana tabacum* cv. Xanthi), cDNA of tomato (*Solanum lycopersicum* cv. Heinz) and potato (*Solanum tuberosum*), respectively. To silence *NRC2/3/4*, 285 bp of *NbNRC2*, 334 bp of *NbNRC3* and 272 bp of *NbNRC4* were combined by overlap PCR and then overlapped fragment was put into pTRV2-LIC vector. For RNLs silencing, a 283 bp of *NbNRG1* and 329 bp of NbADR1 were combined by overlap PCR and then overlapped fragment was cloned into TRV2-LIC vector. The primers used in the PCR are list in (*SI Appendix*, Table S5).

Site-directed and motif-swap mutagenesis

The N-terminal motif swap mutants and site-directed mutants were generated using the specific primers carrying the mutations. The amplified fragments for tag fusion proteins were cloned into pCAMBIA2300-3xFLAG-LIC, pCAMBIA2300-eGFP-LIC vector using ligation-independent cloning method.

Disease resistance assay

For PVX:GFP co-expression, *A. tumefaciens* GV3101 carrying the PVX:GFP-expressing binary vector was coinfiltrated with G10-CCs, G10-NLRs and Pvr4/NIb. After 30 hpi, intensity of GFP fluorescence was measured by using closed FluorCam (Photon Systems Instruments, Czech Republic) with GFP filter to quantify PVX replication.

Agrobacterium-mediated transient overexpression in *N. benthamiana*

A. tumefaciens GV3101 strains carrying the various constructs are prepared for transient overexpression. Agrobacteria were grown overnight at 28°C in LB media supplemented with kanamycine (50 µg/ml) and rifampicin (50 µg/ml). The cultures were precipitated and resuspended in infiltration buffer (10 mM MES (pH 5.6) and 10 mM $MgCl_2$ with 150 µM Acetosyringone) at optical density at 600 nm ($O.D_{600}$) = 0.3 for CC domains or 0.6 for full length NLRs and R genes. For screening of G10-CCs from tomato, tobacco, potato and rice, those were coexpressed with the gene silencing suppressor, p19 (Final $O.D_{600}$=0.25). Agrobacterial suspensions were infiltrated on the abaxial leaves of 4-week-old *N. benthamiana* plants with a needleless syringe. Macroscopic cell death phenotypes were detected by fluorescence-labeled organism bioimaging instrument (FOBI) system (Neoscience, Korea). Strength of cell death was reflected by quantum yield (FV/FM) using closed FluorCam (Photon Systems Instruments, Czech Republic).

Virus-induced gene silencing (VIGS)

VIGS was performed in *N. benthamiana* as described by Liu et al., 2002 (55). A suspension of pTRV1 and pTRV2 carrying a target gene fragment were mixed in a 1:1 ratio in infiltration buffer at final optical density at 600 nm ($O.D_{600}$) = 0.15 respectively. Two leaves of 2-

week old *N. benthamiana* seedlings were infiltrated with Agro suspension mixture. Three weeks later, upper leaves were used for the experiments. and collected to confirm the silencing of the target gene.

Gene expression assay

Total RNA was extracted using TRIzol reagent (MRC, OH, USA) and complementary DNA was synthesized using Superscript II (Invitrogen, CA, USA). Gene-specific primers were used in quantitative RT-PCR at 95 □ for 5 min, followed by 40 cycles with denaturation at 95 □ for 15s, 55 □ for 1 min. qRT-PCR was performed by CFX96 Real time PCR machine (BioRad, USA) with sssoadvanced universal SYBR green supermix (Bio-Rad, USA). Nucleotide sequences of all primers used in this study are listed in (*SI Appendix*, Table S5). The level of gene transcripts was normalized to that of elongation factor gene, *NbEF1-α*.

Confocal laser scanning microscopy

Cells expressing GFP-tagged proteins were examined with a Leica confocal microscope SP8X (Leica Microsystem, Germany) with 40x/1.0 water dipping objective. GFP was imaged using 488 nm excitation and its emission signal was detected from 500 nm to 530 nm. Simultaneous excitation of GFP and plasma membrane marker dye, FM4-64 (Invitrogen, CA, USA) was performed using the 488 nm excitation and emission signal was collected at 500-530 nm and 600-650 nm for GFP and FM4-64, respectively.

DAB staining

Accumulation of hydrogen peroxide (H_2O_2) was detected with 3,3'-Diaminobenzidine (DAB) staining. *N. benthamiana* leaves were detached and incubated in DAB-HCl solution (1 mg/mL, pH 3.8) for overnight at 25°C in the dark. After staining, the leaves were soaked in 95% ethanol to remove chlorophyll.

Immunoblot analysis

50 mg of *N. benthamiana* leaf tissue was ground into fine powder in liquid nitrogen and homogenized in 200 μL of extraction buffer (50 mM Tris-HCl (pH 7.5), 100 mM NaCl, 1 mM EDTA, 1% (v/v) IGEPAL CA-630, 10 % glycerol, 5 mM DTT, 1 mM NaF, 1mM PMSF, 1x EDTA-free protease inhibitor cocktail (Roche)). The lysates were cleared by centrifugation at 12,000 g for 10 min at 4°C. Samples were loaded on a 8 or 10% SES-PAGE gel and detected after blotting with anti-FLAG M2 antibody (SIGMA) (1:10,000 dilution) or anti-HA (Abcam) (1:5,000 dilution).

Quantification and statistical analysis

Statistical analysis and generation of graph were performed using Prism7 (GraphPad). Error bars in all of the figures represent standard deviations of mean. Number of replicates is reported in the figure legends. Statistical comparison among different samples is carried out by one-way or two-way ANOVA with Sidak's multiple comparisons or Dunnett's multiple comparisons. Samples with statistically significant differences are marked with an asterisk or letters.

Acknowledgments

D.C, and H.-Y.L. designed the research. H.-Y.L., E.-H.C, Y.-E.S, and S.O. performed research. H.-Y.L. Y.-E.S. S.B.K, Dr. Hyun-Ah Lee, Y.-E.S., Jihyun Kim, and Haeun Kim constructed plasmids for NLR and NTD screening. H.-Y.L. H.M. and D.C wrote the article with comments from other authors. This work was supported by the National Research Foundation of Korea (NRF) grant funded by the Korea government (MSIT) (No. 2018R1A5A1023599 (SRC) and 2018R1A2A1A05019892).

References

1. J. L. Dangl, D. M. Horvath, B. J. Staskawicz, Pivoting the plant immune system from dissection to deployment. *Science* **341**, 746-751 (2013).
2. P. N. Dodds, J. P. Rathjen, Plant immunity: towards an integrated view of plant-pathogen interactions. *Nat Rev Genet* **11**, 539-548 (2010).
3. P. Moffett, G. Farnham, J. Peart, D. C. Baulcombe, Interaction between domains of a plant NBS-LRR protein in disease resistance-related cell death. *Embo J* **21**, 4511-4519 (2002).
4. J. Wang *et al.*, Ligand-triggered allosteric ADP release primes a plant NLR complex. *Science* **364** (2019).
5. V. Bonardi, K. Cherkis, M. T. Nishimura, J. L. Dangl, A new eye on NLR proteins: focused on clarity or diffused by complexity? *Curr Opin Immunol* **24**, 41-50 (2012).
6. X. Meng, S. Zhang, MAPK cascades in plant disease resistance signaling. *Annu Rev Phytopathol* **51**, 245-266 (2013).
7. F. Jacob, S. Vernaldi, T. Maekawa, Evolution and Conservation of Plant NLR Functions. *Front Immunol* **4**, 297 (2013).
8. H. Adachi, L. Derevnina, S. Kamoun, NLR singletons, pairs, and networks: evolution, assembly, and regulation of the intracellular immunoreceptor circuitry of plants. *Curr Opin Plant Biol* **50**, 121-131 (2019).
9. A. M. Catanzariti *et al.*, The AvrM effector from flax rust has a structured C-terminal domain and interacts directly with the M resistance protein. *Mol Plant Microbe Interact* **23**, 49-57 (2010).
10. K. V. Krasileva, D. Dahlbeck, B. J. Staskawicz, Activation of an Arabidopsis resistance protein is specified by the in planta association of its leucine-rich repeat domain with the cognate oomycete effector. *Plant Cell* **22**, 2444-2458 (2010).
11. I. M. Saur *et al.*, Multiple pairs of allelic MLA immune receptor-powdery mildew AVRA effectors argue for a direct recognition mechanism. *Elife* **8** (2019).
12. L. Rodriguez-Moreno, Y. Song, B. P. Thomma, Transfer and engineering of immune receptors to improve recognition capacities in crops. *Curr Opin Plant Biol* **38**, 42-49 (2017).
13. H. Jin *et al.*, NPK1, an MEKK1-like mitogen-activated protein kinase kinase kinase, regulates innate immunity and development in plants. *Dev Cell* **3**, 291-297 (2002).
14. Y. Zhang, S. Dorey, M. Swiderski, J. D. Jones, Expression of RPS4 in tobacco induces an AvrRps4-independent HR that requires EDS1, SGT1 and HSP90. *Plant J* **40**, 213-224 (2004).
15. S. B. Saucet *et al.*, Two linked pairs of Arabidopsis TNL resistance genes independently confer recognition of bacterial effector AvrRps4. *Nat Commun* **6**, 6338 (2015).
16. C. H. Wu *et al.*, NLR network mediates immunity to diverse plant pathogens. *Proc Natl Acad Sci U S A* **114**, 8113-8118 (2017).
17. J. D. G. Jones, J. L. Dangl, The plant immune system.

Nature **444**, 323-329 (2006).
18. B. C. Meyers, A. Kozik, A. Griego, H. Kuang, R. W. Michelmore, Genome-wide analysis of NBS-LRR-encoding genes in Arabidopsis. *Plant Cell* **15**, 809-834 (2003).
19. J. R. Peart, P. Mestre, R. Lu, I. Malcuit, D. C. Baulcombe, NRG1, a CC-NB-LRR protein, together with N, a TIR-NB-LRR protein, mediates resistance against tobacco mosaic virus. *Current Biology* **15**, 968-973 (2005).
20. V. Bonardi *et al.*, Expanded functions for a family of plant intracellular immune receptors beyond specific recognition of pathogen effectors. *Proc Natl Acad Sci U S A* **108**, 16463-16468 (2011).
21. S. M. Collier, L. P. Hamel, P. Moffett, Cell death mediated by the N-terminal domains of a unique and highly conserved class of NB-LRR protein. *Mol Plant Microbe Interact* **24**, 918-931 (2011).
22. B. Castel *et al.*, Diverse NLR immune receptors activate defence via the RPW8-NLR NRG1. *New Phytol* **222**, 966-980 (2019).
23. T. S. Mucyn *et al.*, The tomato NBARC-LRR protein Prf interacts with Pto kinase in vivo to regulate specific plant immunity. *Plant Cell* **18**, 2792-2806 (2006).
24. J. Ade, B. J. DeYoung, C. Golstein, R. W. Innes, Indirect activation of a plant nucleotide binding site-leucine-rich repeat protein by a bacterial protease. *Proc Natl Acad Sci U S A* **104**, 2531-2536 (2007).
25. T. M. Burch-Smith *et al.*, A novel role for the TIR domain in association with pathogen-derived elicitors. *Plos Biol* **5**, 501-514 (2007).
26. M. A. Sacco, S. Mansoor, P. Moffett, A RanGAP protein physically interacts with the NB-LRR protein Rx, and is required for Rx-mediated viral resistance. *Plant J* **52**, 82-93 (2007).
27. P. Mestre, D. C. Baulcombe, Elicitor-mediated oligomerization of the tobacco N disease resistance protein. *Plant Cell* **18**, 491-501 (2006).
28. M. Bernoux *et al.*, Structural and functional analysis of a plant resistance protein TIR domain reveals interfaces for self-association, signaling, and autoregulation. *Cell Host Microbe* **9**, 200-211 (2011).
29. T. Maekawa *et al.*, Coiled-coil domain-dependent homodimerization of intracellular barley immune receptors defines a minimal functional module for triggering cell death. *Cell Host Microbe* **9**, 187-199 (2011).
30. L. W. Casey *et al.*, The CC domain structure from the wheat stem rust resistance protein Sr33 challenges paradigms for dimerization in plant NLR proteins. *Proc Natl Acad Sci U S A* **113**, 12856-12861 (2016).
31. L. P. Hamel *et al.*, The Chloroplastic Protein THF1 Interacts with the Coiled-Coil Domain of the Disease Resistance Protein N' and Regulates Light-Dependent Cell Death. *Plant Physiol* **171**, 658-674 (2016).
32. J. Wang *et al.*, Reconstitution and structure of a plant NLR resistosome conferring immunity. *Science* **364** (2019).
33. F. Chiarini, G. Bernardello, Karyotype studies in South American species of Solanum subgen. Leptostemonum (Solanaceae). *Plant Biol (Stuttg)* **8**, 486-493 (2006).
34. E. Seo, S. Kim, S. I. Yeom, D. Choi, Genome-Wide Comparative Analyses Reveal the Dynamic Evolution of Nucleotide-Binding Leucine-Rich Repeat Gene Family among Solanaceae Plants. *Frontiers in Plant Science* **7** (2016).
35. S. B. Kim, H. Y. Lee, S. Seo, J. H. Lee, D. Choi, RNA-Dependent RNA Polymerase (NIb) of the Potyviruses Is an Avirulence Factor for the Broad-Spectrum Resistance Gene Pvr4 in Capsicum annuum cv. CM334. *Plos One* **10** (2015).
36. S. B. Kim *et al.*, Divergent evolution of multiple virus-resistance genes from a progenitor in Capsicum spp. *New Phytol* **213**, 886-899 (2017).
37. S. B. Kim *et al.*, The Coiled-Coil and Leucine-Rich Repeat Domain of the Potyvirus Resistance Protein Pvr4 Has a Distinct Role in Signaling and Pathogen Recognition. *Mol Plant Microbe In* **31**, 906-913 (2018).
38. S. Kim *et al.*, New reference genome sequences of hot pepper reveal the massive evolution of plant disease-resistance genes by retroduplication. *Genome Biol* **18**, 210 (2017).
39. O. C. A. Sukarta, E. J. Slootweg, A. Goverse, Structure-informed insights for NLR functioning in plant immunity. *Semin Cell Dev Biol* **56**, 134-149 (2016).
40. M. Baudin, J. A. Hassan, K. J. Schreiber, J. D. Lewis, Analysis of the ZAR1 Immune Complex Reveals Determinants for Immunity and Molecular Interactions. *Plant Physiol* **174**, 2038-2053 (2017).
41. M. R. Swiderski, D. Birker, J. D. Jones, The TIR domain of TIR-NB-LRR resistance proteins is a signaling domain involved in cell death induction. *Mol Plant Microbe Interact* **22**, 157-165 (2009).
42. N. Ishihama, R. Yamada, M. Yoshioka, S. Katou, H. Yoshioka, Phosphorylation of the Nicotiana benthamiana WRKY8 transcription factor by MAPK functions in the defense response. *Plant Cell* **23**, 1153-1170 (2011).
43. S. Gopalan, W. Wei, S. Y. He, hrp gene-dependent induction of hin1: a plant gene activated rapidly by both harpins and the avrPto gene-mediated signal. *Plant J* **10**, 591-600 (1996).
44. C. Weitzel, H. T. Simonsen, Cytochrome P450-enzymes involved in the biosynthesis of mono- and sesquiterpenes. *Phytochem Rev* **14**, 7-24 (2015).
45. J. Glazebrook, Contrasting mechanisms of defense against biotrophic and necrotrophic pathogens. *Annu Rev Phytopathol* **43**, 205-227 (2005).
46. D. Qi, B. J. DeYoung, R. W. Innes, Structure-function analysis of the coiled-coil and leucine-rich repeat domains of the RPS5 disease resistance protein. *Plant Physiol* **158**, 1819-1832 (2012).
47. H. Adachi *et al.*, An N-terminal motif in NLR immune receptors is functionally conserved across distantly related plant species. *bioRxiv* https://doi.org/10.1101/693291 (2019).
48. A. M. Jones, S. Coimbra, A. Fath, M. Sottomayor, H. Thomas, Programmed cell death assays for plants. *Methods Cell Biol* **66**, 437-451 (2001).
49. T. Wroblewski *et al.*, Genome-wide functional analyses of plant coiled-coil NLR-type pathogen receptors reveal essential roles of their N-terminal domain in oligomerization, networking, and immunity. *Plos Biol* **16**, e2005821 (2018).
50. M. Narusaka *et al.*, RRS1 and RPS4 provide a dual Resistance-gene system against fungal and bacterial pathogens. *Plant J* **60**, 218-226 (2009).
51. B. Day *et al.*, Molecular basis for the RIN4 negative regulation of RPS2 disease resistance. *Plant Cell* **17**, 1292-1305 (2005).
52. K. Seong, E. Seo, m. Li, B. Staskawicz, Evolution of NLR resistance genes with non-canonical N-terminal domains in wild tomato species. *BioRxiv* (2019).
53. S. Kim *et al.*, Genome sequence of the hot pepper

provides insights into the evolution of pungency in Capsicum species. *Nat Genet* **46**, 270-278 (2014).
54. S. K. Oh, S. B. Kim, S. I. Yeom, H. A. Lee, D. Choi, Positive-selection and ligation-independent cloning vectors for large scale in planta expression for plant functional genomics. *Mol Cells* **30**, 557-562 (2010).
55. Y. Liu, M. Schiff, S. P. Dinesh-Kumar, Virus-induced gene silencing in tomato. *Plant J* **31**, 777-786 (2002).

Table 1. Screening of autoactive pepper NLRs and N-terminal domains in *N. benthamiana*

Group	No. assigned NLR	Full-length NLR		N-terminal domain (NTD)	
		No. tested NLR	No. autoactive NLR (%)	No. tested NTD	No. autoactive NTD (%)
TNL	54	49	6 (12.2)	16	2 (12.5)
CNL-G1	75	63	0 (0)	10	0 (0)
CNL-G2	91	81	0 (0)	13	0 (0)
CNL-G3	23	23	0 (0)	8	0 (0)
CNL-G4	32	31	0 (0)	9	0 (0)
CNL-G5	12	12	1(8.3)	4	0 (0)
CNL-G6	26	25	0 (0)	5	0 (0)
CNL-G7	18	16	0 (0)	7	0 (0)
CNL-G8	14	14	0 (0)	6	0 (0)
CNL-G9	48	48	1 (2.1)	9	0 (0)
CNL-G10	34	33	3 (9.1)	24	17 (70.8)
CNL-G11	7	7	1 (14.3)	5	1 (20)
CNL-G12	9	8	0 (0)	5	0
CNL-G13	1	1	0 (0)	1	0
CNL-NG*	25	25	3 (12)	8	2 (25)
Total	469	436	15	131	22

*NG: non-group

*NLR: nucleotide-binding domain and leucine-rich repeat. †NTD: N-terminal domain
‡NG: non-group

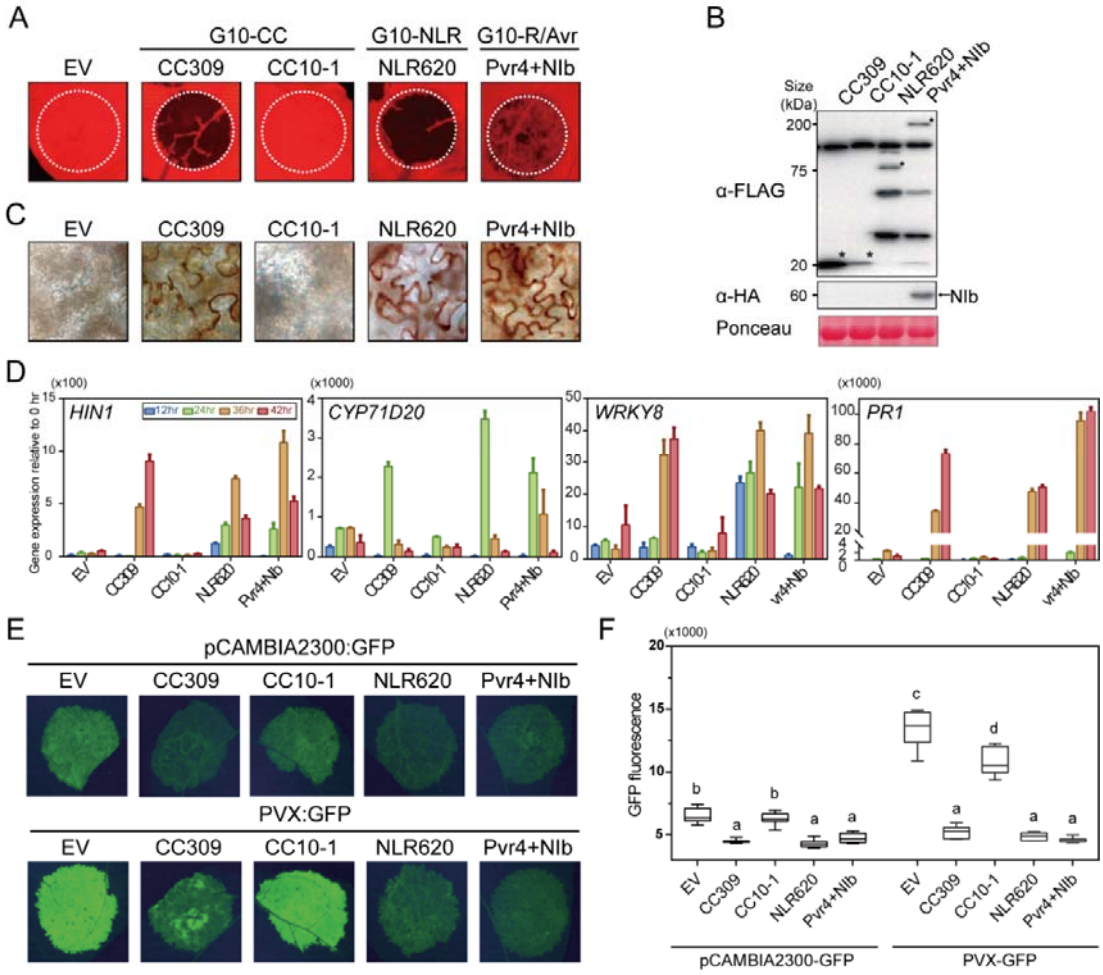

Figure. 1. Autoactive G10-NLR and G10-CC trigger defense-related cell death.

(A) CC309, NLR620, and Pvr4 with its cognate effector NIb induce cell death except CC10-1. EV (empty vector) was used as a negative control. The leaves of four-week-old *N. bentamiana* were infiltrated with agrobacteria harboring each constructs. Images were taken 3 dpi. (B) Protein accumulation was confirmed by immunoblot analysis. Equal protein loading was confirmed by membrane staining by Ponceau S stained membrane. Asterisks indicate the expected band of proteins. (C) H_2O_2 were accumulated in CC309, NLR620, and Pvr4/NIb-infiltrated leaves not CC10-1 and EV. Leaves were stained with 3,3'-diaminobenzidine (DAB) at 2 dpi. N=3. (D) Defense-related genes, *HIN1*, *CYP71D20*, *WRKY8* and *PR1*, were dramatically elevated by CC309, NLR620, and Pvr4/Nib. Four-week-old *N. benthamiana* leaves infiltrated by EV, CC309, CC10-1, NLR620 and Pvr4/NIb were collected at various time points. The data were shown as means ±SD (N=3). (E) and (F) Enhanced resistance to Potato Virus X by CC309, NLR620, and Pvr4/NIb. pCAMBIA2300:GFP or PVX:GFP was co-infiltrated with agrobacteria cells carrying EV, CC309, CC10-1, NLR620 and Pvr4/NIb. (F) Accumulation of GFP was visualized 30 hpi. fluorescence emission of GFP was quantified by a FluorCam with GFP filter. Letter codes indicate statistical differences analyzed by one-way ANOVA with Sidak's multiple comparisons. The above experiments were repeated two times with eight biological replicates.

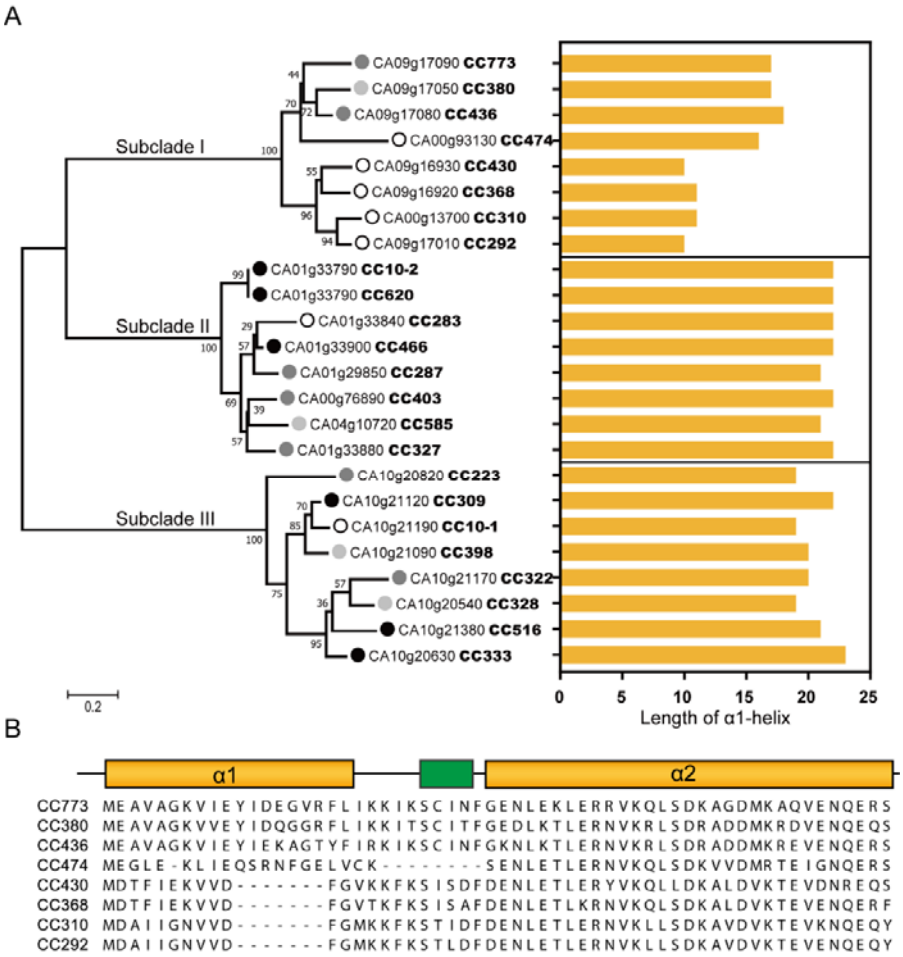

Figure. 2. First α-helix region is critical for autoactivity of G10-CC domains.

(A) Phylogenetic tree of G10-CCs (left) and length of first α-helix (right). Phylogenetic tree was constructed using amino acid sequences of G10-CC domains. Maximum likelihood model was used and bootstrap analysis was performed with 1,000 replicates. The strength of cell death is represented as a grayscale circle at the left side of gene ID (closed circle, strong; dark gray circle, medium; light gray circle, weak cell death; open circle, no cell death). (B) Alignment of CC domains in subclade I and schematic representation of secondary structure of subclade I CC domains. Non-autoactive CC domains (CC474, CC292, CC310, CC368, CC430) are deficient in intact form of first α-helix. α-helix and β sheet are represented yellow and green box respectively.

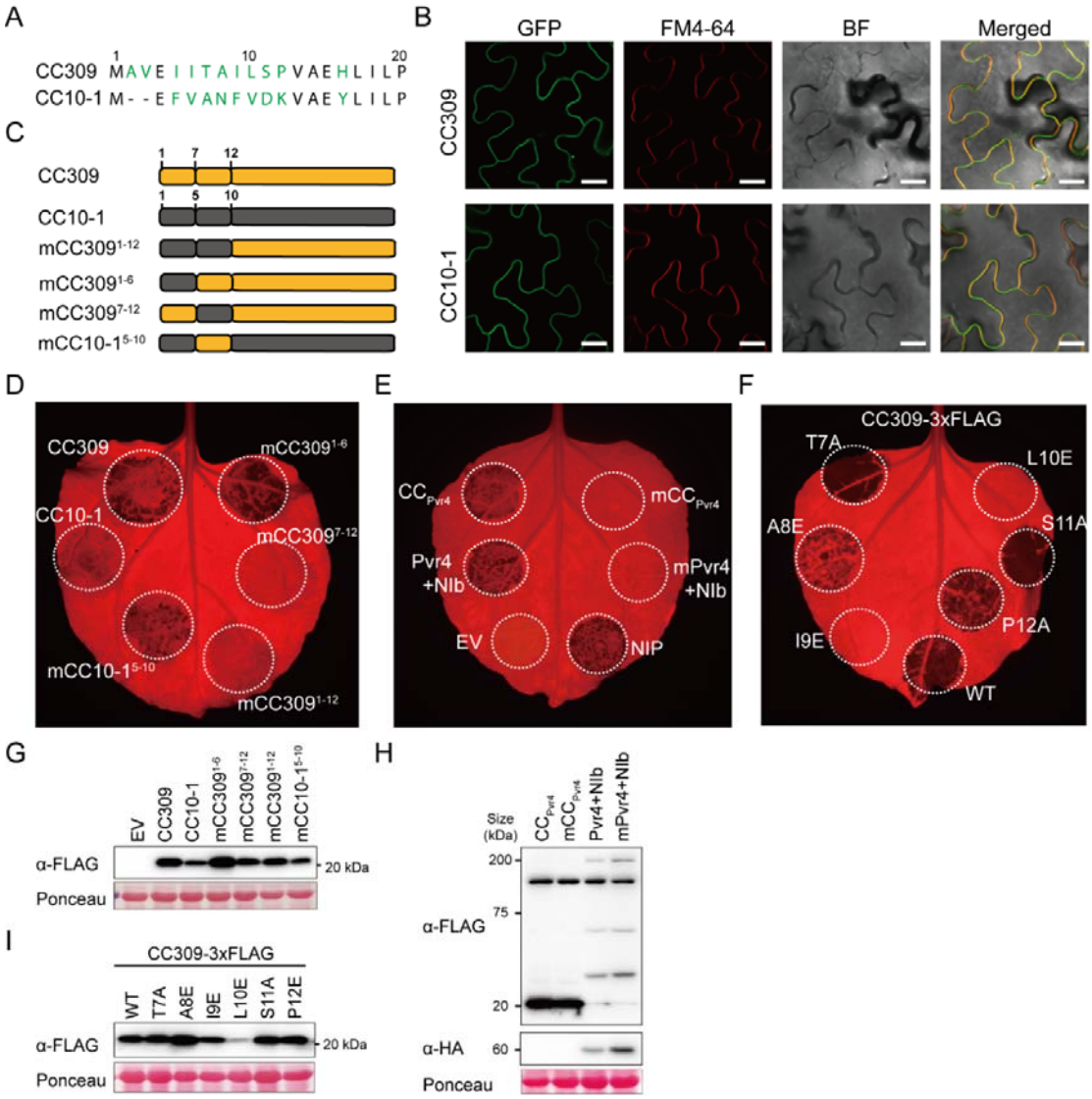

Figure. 3. The N-terminal 'TAILSP' motif in subclade III G10-CCs is critical for autoactivity.

(A) Alignment of N-terminal region of CC309 and CC10-1. Different residues are highlighted in green color. (B) Co-localization of the CC309-GFP and CC10-1-GFP proteins with FM 4-64 labeled plasma membrane. Confocal microscopy images were taken at 26 hpi. Bar=20 μm. (C) Schematic diagram of CC309 N-terminal chimeras with CC10-1. (D) Cell death induced by CC309 mutants and CC10-1 mutant described in (C). mCC10-1$^{5-10}$ (left lower circle) and mCC309$^{1-6}$ (right top circle) contain 'TAILSP' motif. (E) The compromised cell death of defect 'TAILSP' motif in Pvr4 and CC domain of Pvr4 (CC_{Pvr4}). The *Phytophthora sojae* Necrosis□inducing protein (NIP) was used as positive control for cell death. (F) Compromised cell death of I9E (left lower circle) and L10E (right top circle) point mutant on TAILSP motif. All swap or point mutants were transiently expressed in *N. benthamiana* and cell death was visualized after 3 dpi. (G-I) Protein accumulation as described in (D), (E) and (F) respectively, was examined by western blot analysis. Equal protein loading was confirmed by Ponceau S stained membrane. The above experiments were repeated at least three times with similar results.

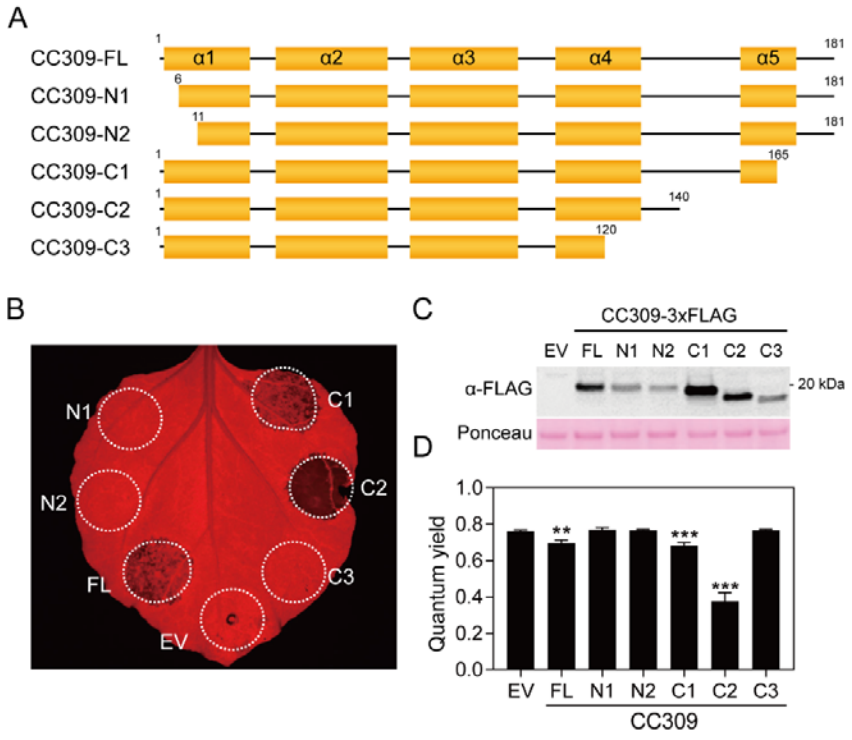

Fig. 4. Four α-helices (α1 to α4) are minimal unit for cell death inducing activity for CC309.

(A) Schematic diagram of CC309 and deletion mutants. Secondary structure of CC309 was predicted by JPRED4. Predicted α-helix is indicated by yellow box. (B) Compromised cell death phenotype of α1 (N1 and N2) or α4 helix (C3). Deletion mutants were transiently expressed in *N. benthamiana* and image was taken at 3dpi. (C) Protein accumulation were analyzed by immunoblot. (D) The strength of cell death was reflected by quantum yield (FV/FM) using closed FluorCam. Significance was determined using one-way ANOVA followed by Dunnett's multiple comparisons, where asterisks represent statistically significant differences: ** $P < 0.01$, *** $P < 0.001$. Data are means (±SD) of four biological replicates.

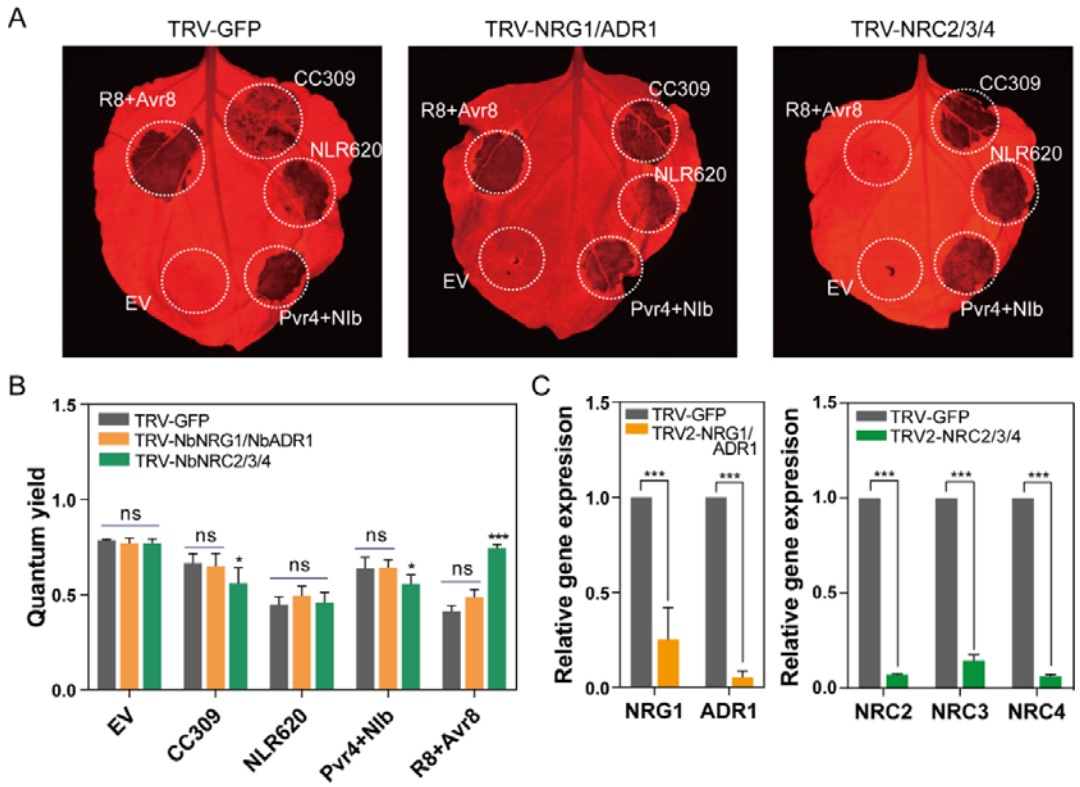

Figure 5. Cell death induced by autoactive G10-CCs or G10-NLRs are independent on *NRG1/ADR1* or *NRCs* type helpers mediated pathway.

(A) Cell death phenotype induced by autoactive CC309, NLR620 and Pvr4 with NIb in *NRG1/ADR1*- or NRC2/3/4- silenced *N. benthamiana*. Agrobacteria carrying each clone were infiltrated 3 weeks after VIGS. NRC2/3/4-dependent *P. infestans* resistance gene R8 and its cognate effector, Avr8 were used as helper dependent control. Each experiment was replicated independently two times (n=10). Leaves were photographed at 3 dpi. (B) The strength of cell death was reflected by quantum yield (Fv/Fm) using closed FluorCam. Significance was determined using one-way ANOVA followed by Dunnett's multiple comparisons, where asterisks represent statistically significant differences: * P <0.05, *** P < 0.0001. Data are means (±SD) of four biological replicates. (C) Relative transcript abundance for each gene was measured by quantitative RT-PCR in silenced plants. The mean values (±SD) for transcript levels were normalized relative to *N. benthamiana EF1-α*. Transcript levels of GFP-silenced plants were set to 1. Error bars represent the mean of three biological replicates and asterisks indicate significant differences at P < 0.0001 with a two-way ANOVA followed by sidak's multiple comparisons.

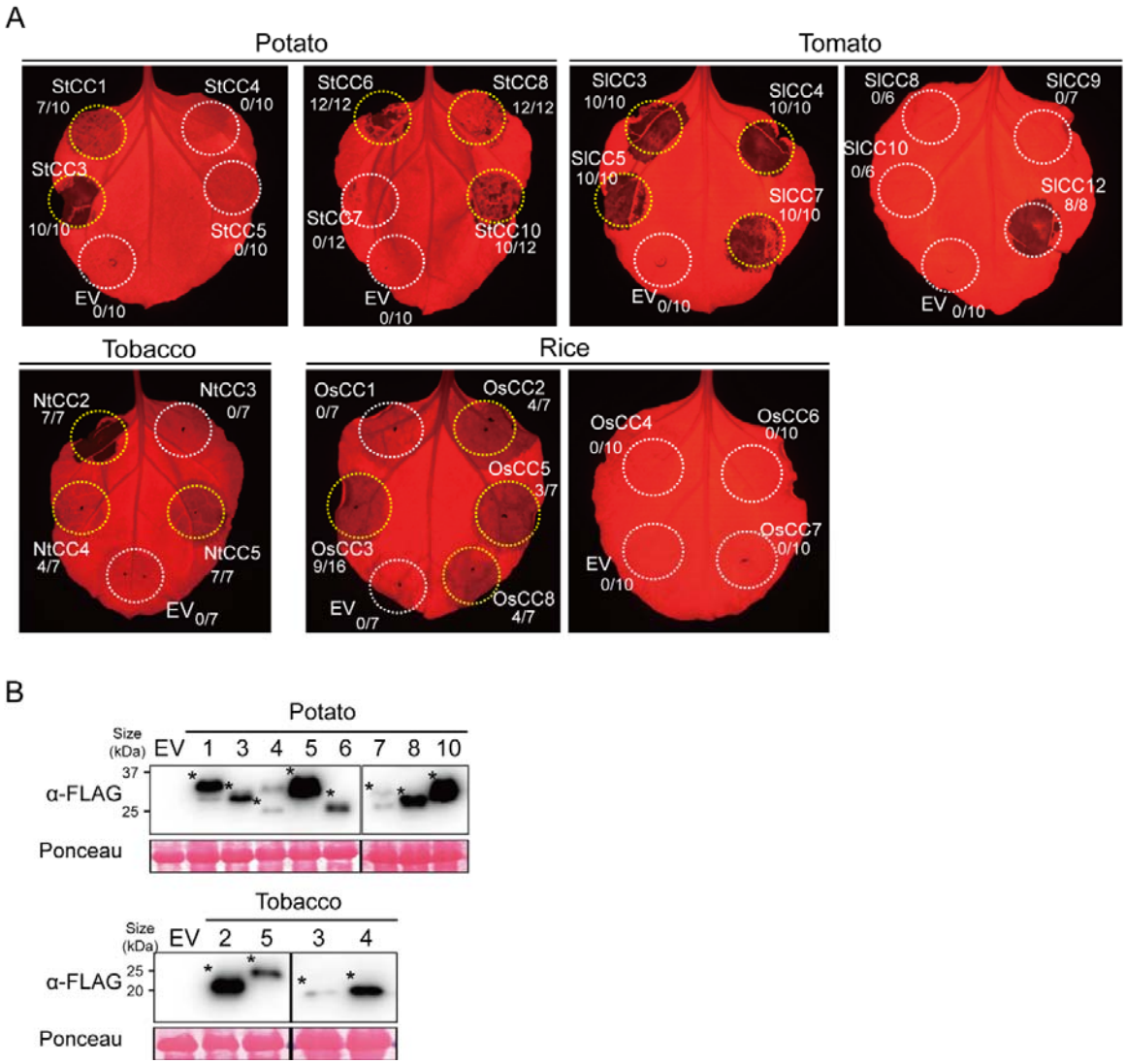

Figure 6. G10-CCs of other Solanaceae and rice plants also induce cell death in *N. benthamiana*.

(A) G10-CCs from Solanaceae plants (potato, tomato and tobacco) and rice were co-expressed with the gene silencing suppressor p19. in *N. benthamiana*. Cell death induced by autoactive CCs are represented in yellow circles. Frequency of cell death induced by G10-CC is presented below. Images were photographed at 3 dpi. The experiments were repeated three times with at least six biological replicates. (B) Protein accumulation were analyzed by immunoblot. Asterisks indicate the expected band of proteins. Equal protein loading was confirmed by Ponceau S stained membrane.